The CYDER Survey: First Results

FRANCISCO J. CASTANDER[1,2,3], EZEQUIEL TREISTER[2,3], JOSÉ MAZA[2], PAOLO S. COPPI[3], THOMAS J. MACCARONE[4], STEPHEN E. ZEPF[5], RAFAEL GUZMÁN[6], MARÍA TERESA RUIZ[2]

[1] Institut d'Estudis Espacials de Catalunya/CSIC, Gran Capità 2-4, 0834 Barcelona, Spain
[2] Departamento de Astronomía, Universidad de Chile, Casilla 36-D, Santiago, Chile
[3] Astronomy Department, Yale University, P.O. Box 208101, New Haven, CT06520, USA
[4] SISSA, via Beirut 2-4, 34014 Trieste, Italy
[5] Department of Physics and Astronomy, Michigan State University, East Lansing, MI 48824, USA
[6] Department of Astronomy, University of Florida, P.O. Box 112055, Gainesville, FL 32611, USA

Received date will be inserted by the editor; accepted date will be inserted by the editor

Abstract. We present the Calán-Yale Deep Extragalactic Research (CYDER) Survey. The broad goals of the survey are the study of stellar populations, the star formation history of the universe and the formation and evolution of galaxies. The fields studied include Chandra deep pointings in order to characterize the X-ray faint populations. Here we present the results on the first fields studied. We find that the redshift distribution is consistent with that found in the Chandra Deep Field North. The distribution of hardness ratios is, however, softer in our sample. We find a high redshift quasar, CXOCY J125304.0-090737 at $z = 4.179$, which suggests that the abundance of low luminosity high redshift quasars may be larger than what would be expected from reasonable extrapolations from the quasar optical luminosity function.

Key words: surveys — quasars: general — galaxies: active — X-rays — galaxies: evolution

1. Introduction: the CYDER Survey

The Calán-Yale Deep Extragalactic Research (CYDER) Survey is a collaborative effort between the Universidad de Chile and Yale University to study in detail faint stellar and extragalactic populations in survey mode. The broad scientific goals are directed towards the core observing goals of the new generation of large optical and millimeter facilities. The program takes full advantage of these facilities by combining deep optical and near-IR photometric and spectroscopic observations on wide field cameras and spectrographs using a wide variety of 4-m and 8-m class telescopes.

1.1. Strategy

Fields were selected at high galactic latitude to minimize the effects of extinction. They were also spread out in right ascension to allow flexibility in the allocation of telescope time. Amongst our fields, we selected fields observed by the Chandra X-ray Observatory satellite with exposure times longer than 50 ks.

Correspondence to: fjc@ieec.fcr.es

The CYDER survey original design goal was to cover 1 square degree down to limiting magnitudes $U \sim 26$, $B \sim 26.5$, $V \sim 26$, $R \sim 25.5$, $I \sim 25$, $z \sim 24$, $J \sim 22$ and $K \sim 20$ at $\mathrm{S/N} \sim 10$. So far, the optical coverage is larger than 1 square degree in some filters while there is no area coverage in others. In the near infrared only 1/2 of a square degree has been imaged. Optical spectroscopy is underway in a few selected fields, while near infrared spectroscopy has not started yet.

2. Observations

The first fields studied were three of the earliest deep Chandra pointings to become publicly available. One of these field is in the Northern hemisphere. It is the Chandra pointing towards the blazar 1156+295. The X-ray exposure time was 75ks. The other two fields are in the South. They were pointing to the Hickson compact group HCG62 (exposure time 50ks) and the blazar Q1127-145 (30ks). These two Southern fields will be the ones discussed in this paper.

2.1. X-ray data

Both the HCG62 and Q1127-145 fields were observed with the Chandra ACIS-S instrument. We retrieved these images from the archive and analyzed them using standard techniques with the CIAO package. In the HCG62 field we detect 34 X-ray sources in the s3 ACIS CCD and 16 sources in the s4. In Chandra pointing towards Q1127-145, the s3 CCD was the only CCD read. It was read in subraster mode and therefore only 5 X-ray sources are detected in that field.

2.2. Optical and Infrared Imaging

We have observed both X-ray fields with the CTIO 4m MOSAIC-II camera. The total integration time for the HCG62 field is 200 minutes in U, 36min in B, 80min in V and 25 min in I under 1.0-1.5" conditions. In the Q1127-145 field the integration times are 80, 75 and 25 minutes in V, R and I respectively. Images were reduced using standard techniques with the IRAF/MSCRED package.

In the near infrared we have observed both fields at Las Campanas Observatory with the DuPont 2.5m telescope using the Wide Field InfraRed Camera during 60 minutes in J and 120 minutes in K_s under typical 0.6-0.7" seeing conditions. We have reduced the data with the IRAF DIMSUM package following standard procedures.

2.3. Optical Spectroscopy

Follow up spectroscopy of these fields was obtained at the ESO Cerro Paranal Observatory with the UT4/Yepun telescope using the FORS2/MXU instrument and at the Las Campanas Observatory with the LDSS-2 instrument at the Magellan Baade telescope. Several masks were designed which included slits for most, but not all, of the X-ray sources in these fields. Masks were observed for approximately two hours. The instrument configuration used resulted in a spectral resolution of $R \sim 520$ at VLT and $R \sim 350$ at Magellan. The spectra were reduced using standard techniques with IRAF and calibrated in wavelength using He-Ar comparison lamps exposures and the night sky lines.

3. First Results

In our first two Southern fields we have spectroscopically identified 25 X-ray sources which corresponds to approximately half of the total X-ray sources detected. Table 1 summarizes the percentages of the different type of objects in our sample. For comparison we also present the results for the Chandra Deep Field North (CDF-N; Brandt et al 2001, Barger et al 2002) and the Chandra Multiwavelength Project (ChaMP; Green et al 2003). We have grouped the different object types in broad classes and have translated the source types of Barger et al (2002) into these types. The CDF-N, CYDER and ChaMP surveys reach different X-ray flux limits; the CDF-N survey reaching the faintest, the ChaMP survey, the brightest. Table 1 demonstrates how the source composition changes with flux limit in an X-ray survey, although the identification incompleteness may hide or enhance certain trends. At bright flux limits, the broad line active galactic nuclei/quasars dominate the extragalactic sources. Their percentage contribution diminishes as the flux limit lowers due to the appearence of a new population of X-ray fainter narrow emission lines AGN/QSOs and normal galaxies.

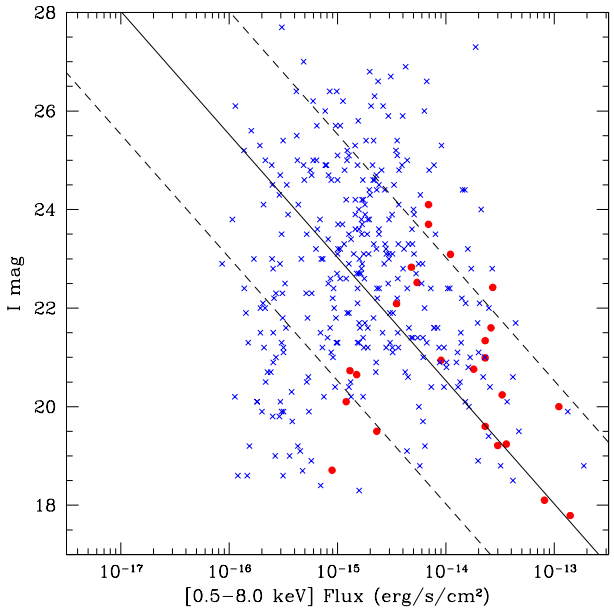

Fig. 1. I magnitude plotted against full band (0.5-8.0 keV) X-ray flux. Blue crosses represent the CDF-N sources and red circles, the CYDER sources. The black solid line represents the line of constant X-ray-to-optical flux ratio, that is, objects with $f_I/f_x = 1$, where f_I is the flux in the I optical band and f_x the X-ray flux. The two dashed lines correspond to objects with $\log(f_I/f_x) = \pm 1$, enclosing the region populated by *normal* AGN/QSOs

Table 1. Approximate percentages of different type of sources in the CDF-N (Barger et al 2002), the CYDER and ChaMP (Green et al 2003) surveys

	CDFN	CYDER	ChaMP
Stars	5%	5%	10%
Broad line AGN/QSO	25%	40%	65%
Narrow line AGN/QSO	50%	40%	15%
Galaxies	20%	15%	10%
Total Number of Identified Sources	170	25	∼200
Total Number of Detected Sources	370	55	-

Figure 1 shows the I band and total X-ray flux of our Chandra sources. For comparison we also plot the CDF-N sources. In our sample we find that approximately 30% of our sources do not show an optical counterpart down to $I \sim 24$. In the case of the CDF-N 16% are undetected down to $I \sim 26$ and 35% down to $I \sim 24$. Overall, the distribution of our sources in the I .vs. X-ray flux plane occupy the same parameter space as the CDF-N sources cut at our same X-ray flux limit.

We compare the CYDER and CDF-N source redshift distributions in Figure 2. A Kolmogorov-Smirnov (KS) test

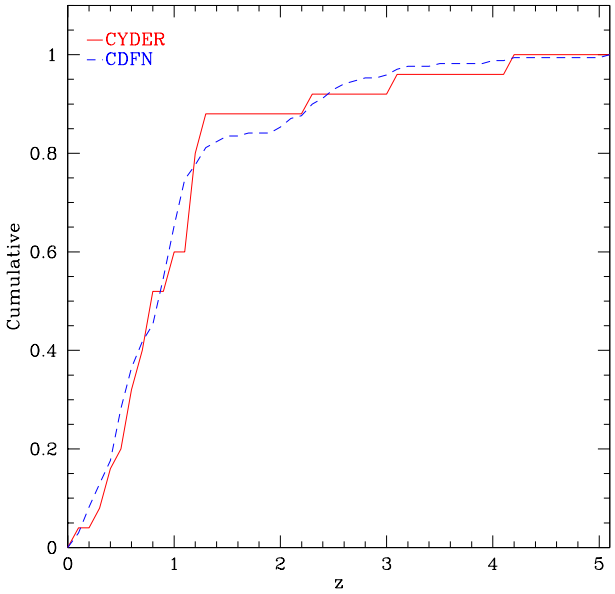

Fig. 2. Cumulative redshift distribution of CYDER (solid red) and CDF-N (dashed blue) sources.

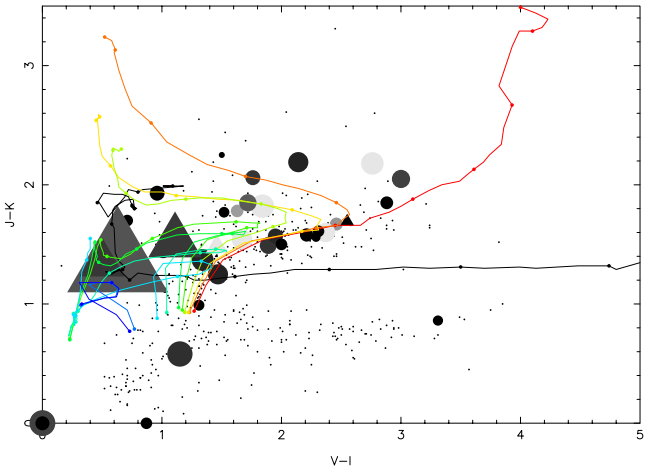

Fig. 3. $J-K$ .vs. $V-I$ colour-colour plot including the CYDER X-ray sources. The small dots represent the colours of the objects in a reduced area of our optical and near infrared coverage of our Chandra fields. The main sequence stars (band of objects from $J-K\sim 0.3$ and $V-I\sim 0.6$ to $J-K\sim 0.8$ and $V-I\sim 3.5$) nicely separate from the rest of the extragalactic sources. The grey symbols indicate the X-ray sources (circles: sources in the HCG62 field; triangles: Q1127-145 field). The size of the circles and triangles is proportional to the X-ray flux. The grey intensity of the symbols shows the hardness ratio. The softest sources (HR=-1) are represented in dark grey and the hardest sources (HR=1) in light grey. The black line indicates the expected location of a QSO at different redshifts. The small dots in the line indicate separations of 0.5 units in redshift. The track starts at $z=0$ at $J-K\sim 1.9$ and $V-I\sim 1.1$, then moves blue-wards in $V-I$ at approximately constant $J-K$ up to $z\sim 2$, then moves blue-wards in $J-K$ at approximately constant $V-I$ up to $z\sim 3-3.5$ and finally quickly moves red-wards in $V-I$ at approximately constant $J-K$. The grey (coloured in electronic version) tracks represent the expected evolutionary path of different galaxy types. The dark grey curve most to the right (red) is a 1 Gyr burst of star formation occurring 15 Gyr ago that evolves passively since. The other evolutionary tracks are computed with star formation prescriptions that broadly reproduce the observed photometric properties of E, S0, Sa, Sb, Sbc, Sc, Sd and irregular galaxies (from right to left run from earlier types to later types). The points at the bluest $J-K$ colour in each track represent those galaxies at $z=0$. Small dots on the tracks are then spaced in 0.5 units in redshift.

shows that both distribution are compatible with having been drawn from the same parent population and are therefore statistically indistinguishable. Given that the CDF-N sources are typically fainter, we have cut their sample at the effective X-ray flux limit of our sample. If we compare the redshift distribution in this case, they remain to be statistically compatible. It is worth noting that in our sample there are 5 QSOs at a redshift $z\sim 1.2$ in the same field. This large scale structure feature is noticeable in our redshift distribution and stresses the need to study sufficient sources and fields as to not be biased by such structures.

We have also compared the X-ray properties of our sample to the CDF-N sources. We find that our sources are in general softer than those in the CDF-N (see Treister & Castander 2003). A KS test indicates that the hardness ratio distributions are incompatible with being drawn from the same parent population. This results may be expected as the CDF-N sources are typically fainter and fainter sources are in general harder (e.g., Giacconi et al 2001; Tozzi et al 2001; Brandt et al 2001; Stern 2002). However, if we impose our effective flux limit to the CDF-N sample we still find that our sources are significantly softer than the reduced brighter CDF-N subsample.

We also investigate what the optical properties of our sample are. Figure 3 is a colour-colour plot including our X-ray sources counterparts (see the figure caption for an explanation of the symbols). Two sources lie on the stellar locus. One is spectroscopically identified as a star, while the other has not been observed spectroscopically. The rest of the sources populate the region of colour-colour space of extragalactic sources. Some of our broad emission line AGN/QSOs are close to the expected location of typical quasars. Others, on the other hand, deviate from their expected position indicating that they are probably reddened. The majority (although not all) of our soft sources lie close to the expected locus of early-type galaxies. The hardest sources populate the regions of mildly active galaxies at redshifts $z\sim 0.5-1.0$. They may be at such locations because they are indeed this type of galaxies or because they have been reddened to that part of colour-colour space.

We compare the photometric and X-ray properties of our sources. We find that the hardest sources are preferentially redder than the rest of the objects. However, we also find soft sources that are red, implying that while blue sources are preferentially soft, red sources can be either X-ray hard or soft. Given the reduced number of sources in our sample, this effect could simply be a statistical fluctuation.

The spectra of our sources reveal a diverse variety of type of objects. We find typical examples of broad and narrow emission line AGN/QSOs. We find typical old stellar population spectral energy distributions. There are also examples

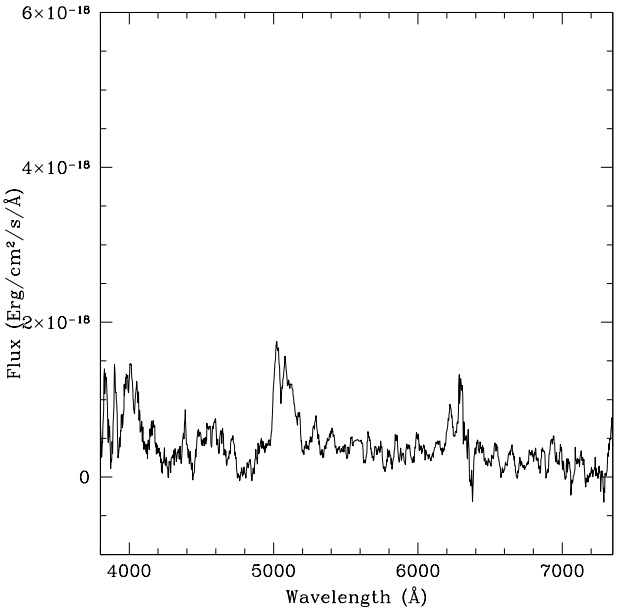

Fig. 4. Optical spectrum of CXOCY J125241.0-091622 obtained at UT4/Yepun VLT.

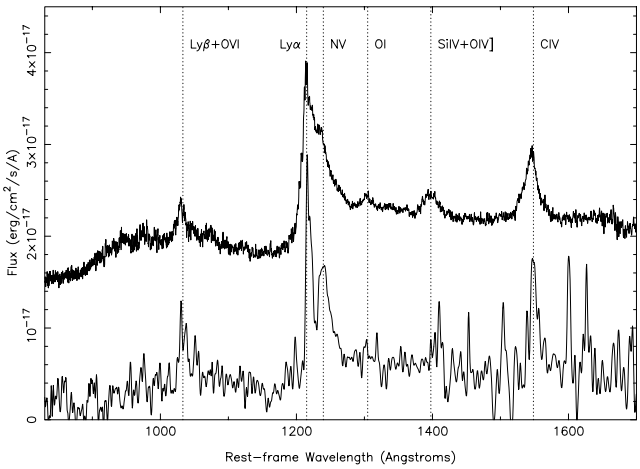

Fig. 5. Optical spectrum of CXOCY J125304.0-090737 obtained at UT4/Yepun VLT. For comparison, we also show the error weighted average of the SDSS Early Data Release QSO spectra at $z > 4$. This composite spectrum have arbitrary zero point and scaling offsets for display purposes and it is shown above the spectrum of CXOCY J125304.0-090737. The most common QSO emission lines are indicated as dotted lines. The emission lines in CXOCY J125304.0-090737 are narrower than the typical SDSS spectrum.

of poststarburst galaxies and objects whose spectral classification is difficult as they have broad emission lines typical of quasars and spectral characteristics of old stellar population with some moderate on-going star formation. Some of our objects show obvious signs of strong absorption.

Here we comment on two of our X-ray sources. CXOCY J125241.0-091622 is a quasar at redshift $z = 2.282$ (Figure 4) with a harder than usual X-ray spectrum $\Gamma \sim 1.3$. In the optical its $V - K$ color is 4.0 which is one magnitude redder than the expected colour of a prototype quasar at this redshift (Figure 3). Both X-ray and optical data thus indicate that this is an obscured object. Such objects are predicted in models as contributors to the X-ray Background at faint fluxes.

CXOCY J125304.0-090737 is an optically faint quasar ($M_B = -23.69 + 5 \times log(h_{65})$) with a typical QSO spectrum (figure 5). In X-rays, CXOCY J125304.0-090737 is also X-ray faint ($f_X = 1.7 \pm 0.4 \times 10^{-15}$ ergs s^{-1} cm^{-2} in the [0.5-2.0] keV band) with a somewhat harder spectrum ($\Gamma \sim 1.7$ or $HR \sim -0.35$) than typical low redshift or high redshift optically selected quasars. We speculate that a reflection component can slightly harden the spectrum but by no means is this the only mechanism. CXOCY J125304.0-090737 X-ray-to-optical emission is X-ray strong ($\alpha_{ox} \sim -1.35$) compared to high redshift optically selected quasars (see Castander et al 2002 for further details).

CXOCY J125304.0-090737 is the only quasar above $z = 4$ found so far in the CYDER survey. However, the space density implied by its discovery is higher than reasonable extrapolations of the quasar optical luminosity function to fainter luminosities at high redshifts (Fan et al 2001) . Although this object by itself does not constrain the faint end of the luminosity function at high redshift, it demonstrates the possibilities that X-ray surveys have to achieve this goal.

4. Summary

We have briefly presented the CYDER survey, which is currently underway. We have focused in the first fields studied that were chosen to coincide with moderately deep Chandra X-ray pointings. We have investigated the nature of the X-ray sources in these fields. We find that the broad X-ray and optical properties of our sources are similar to the ones studied in the CDF-N. The only difference is that our sources appear to be softer. We also stress the fact that our X-ray sources are of diverse optical spectral types and have highlighted the discovery of a high redshift X-ray selected quasar.

The current X-ray surveys (most of which are presented in this volume) that have flourished with the launch of the new X-ray observatories promise to be key to our understanding of the faint X-ray populations. The CYDER survey will be one of the surveys contributing to pin down the evolution of accretion material on to black holes which seems to be closely related to the star formation history of the universe.

Acknowledgements. We acknowledge the financial support received from the Fundación Andes that has enabled the collaboration between the Universidad de Chile and Yale University and therefore has made the CYDER survey possible.

References

Barger, A. J. et al.: 2002, AJ, 124, 1839
Brandt, W. N. et al.: 2001, AJ, 122, 2810
Castander, F. J. et al.: 2002, AJ, submitted
Giacconi, R. et al.: 2001, ApJ, 551, 624
Green, P.J. et al: 2003: AN, this volume
Fan, X. et al: 2001, AJ, 121, 31
Stern, D. et al.: 2002, AJ, 123, 2223
Tozzi, P. et al.: 2001, ApJ, 562, 42
Treister, E. & Castander, F. J.: 2003, AN, this volume